

Metal-insulator transition and charge-density wave in $\text{Fe}_{0.25}\text{Nb}_{0.75}\text{Se}_3$

S. J. Hillenius and R. V. Coleman

Department of Physics, University of Virginia, Charlottesville, Virginia 22901

R. M. Fleming and R. J. Cava

Bell Laboratories, Murray Hill, New Jersey 07974

(Received 26 August 1980)

The compound $\text{Fe}_x\text{Nb}_{1-x}\text{Se}_3$, which has been prepared in the form of single crystals and powders, only forms in a narrow range of stoichiometry near $x = 1/4$. The crystal structure of NbSe_3 is radically modified by the addition of iron and contains four chains of metal atoms per unit cell, rather than six, as in the pure material. The resistance of $\text{Fe}_{0.25}\text{Nb}_{0.75}\text{Se}_3$ rises by nine orders of magnitude as the temperature is lowered from 120 to 2.8 K, although at room temperature the resistivity is comparable to pure NbSe_3 . At temperatures below 19 K, the resistance rise is reasonably well described by the expression $\rho = C \exp(T_0/T)^{1/4}$, characteristic of a Mott or Anderson type of metal-insulator transition. X-ray studies show the formation of an incommensurate charge-density-wave superlattice below ~ 140 K. This can enhance the metal-insulator transition and indicates that the Fermi-surface instability is an extremely dominant feature in compounds of the NbSe_3 type. The absence of a superlattice at room temperature indicates that the iron is randomly substituted in either two or four of the Nb-atom chains.

I. INTRODUCTION

The transition-metal trichalcogenide, NbSe_3 , is an anisotropic linear-chain material which exhibits a number of unusual transport properties. Chief among these is the observation of nonlinear conductivity¹ associated with two independent charge-density-wave (CDW) phase transitions^{2,3} at 144 and 59 K. The nonlinear behavior is now believed to be a result of a current-carrying or "sliding-mode" CDW, which is pinned to the lattice by impurities but can be depinned by the application of a small electric field.^{3,4} In addition to studies of pure NbSe_3 , the interpretation of a current-carrying CDW is also supported by an investigation of the nonlinear conductivity as a function of impurity doping.⁵ The impurity studies show that a modest substitution of Ta or Ti for the niobium results in stronger pinning of the CDW to the lattice.

In this paper, we present the results of electron transport and structural studies of iron-doped NbSe_3 , and the data show a dramatic departure from both the chemical and the physical properties of the pure material. Contrary to the case of Ta or Ti doping, the compound $\text{Fe}_x\text{Nb}_{1-x}\text{Se}_3$ can only be prepared with $x = \frac{1}{4}$. Single crystals of $\text{Fe}_{0.25}\text{Nb}_{0.75}\text{Se}_3$ show a striking nine-orders-of-magnitude increase in the resistance as the temperature is lowered. In the range 2.8 to 19 K, the data can be fit with a function of the form $\rho \propto \exp(T^{-1/4})$. X-ray scattering at low temperatures shows a weak, incommensurate lattice distortion with a reduced wave vector of about $\vec{q} = (0, 0.26, 0)$ which forms at 140 K. This can be contrasted with pure NbSe_3 which has two in-

dependent CDWs with reduced wave vectors of $\vec{q}_1 = (0, 0.243, 0)$ and $\vec{q}_2 = (0.5, 0.263, 0.5)$. Room-temperature structural studies show the new compound has the same morphology and diffraction symmetry as pure NbSe_3 . The iron is incorporated randomly in the lattice, and the metal atoms apparently retain their trigonal coordination. In contrast to the six prismatic chains found in NbSe_3 , the unit cell of $\text{Fe}_{0.25}\text{Nb}_{0.75}\text{Se}_3$ contains four chains. Magnetic susceptibility shows no evidence of ferromagnetic ordering and very little evidence of magnetic-moment formation.

The fact that the CDW and large resistance rise appear at approximately the same temperature and the evidence showing the iron is uniformly incorporated into the lattice in random metal sites, suggests that a Mott type of localization, enhanced by the CDW, may be causing the resistance rise. A similar mechanism has been proposed for the low-temperature insulating behavior of the layered compounds $IT-M_x\text{Ta}_{1-x}\text{S}$ and $IT-M_x\text{Ta}_{1-x}\text{Se}_2$, with $M = \text{Fe}, \text{Ni}, \text{or Co}$.⁶

II. EXPERIMENTAL TECHNIQUES

Both single crystals and powder samples of $\text{Fe}_{0.25}\text{Nb}_{0.75}\text{Se}_3$ were prepared using the same procedure described previously for pure NbSe_3 .⁷ In each case, stoichiometric amounts of the elements were sealed in evacuated quartz tubes. For the powder samples, the tubes were uniformly heated to 650 °C for one or two days. For single crystals a temperature gradient of about 650–700 °C was maintained for about two weeks. Fibrous, needlelike crystals which look identical

to pure NbSe₃, grow in the cooler portions of the tube.

The stoichiometry of the single-crystal specimens was analyzed with a scanning electron microscope employing energy analysis of the x-ray fluorescence. These results indicate that the compound Fe_xNb_{1-x}Se₃ can be prepared only over a narrow range of stoichiometry, near $x = \frac{1}{4}$. For single crystals prepared from bulk material with $x < 0.10$, no iron was detected by x-ray fluorescence. Instead of the large increase in resistance at low temperature seen in Fe_{0.25}Nb_{0.75}Se₃, these crystals show CDW anomalies characteristic of pure NbSe₃ but low resistance ratios, ($R_{273\text{ K}}/R_{4.2\text{ K}} \approx 10$, in the same range as lightly doped Ta_xNb_{1-x}Se₃). For $x < 0.10$, the magnetic susceptibility shows a moment at low temperatures which would correspond to about 0.01% iron if the iron were assumed to have an effective moment of between two and four. At room temperature the susceptibility is weakly diamagnetic, as is pure NbSe₃.

For starting materials with more than 10% iron, the resulting crystals all showed the rapid resistance rise below 100 K and energy analysis of the x-ray fluorescence of these crystals showed them to all be of the same composition. The composition was determined by comparing the amplitude of the $L\alpha$ peaks for these crystals with crystals of pure NbSe₃ and NbSe₂. The ratio of the Se($L\alpha$) peaks was compared for all three compounds and it was determined that the ratio of Nb to Se for the Fe_xNb_{1-x}Se₃ crystals was 0.24 ± 0.01 . The iron concentration was determined by comparing the Fe ($K\alpha$) and Se($K\alpha$) peaks for the Fe_xNb_{1-x}Se₃ crystals and Fe_{0.05}NbSe₂ crystals. This was done to compensate for matrix effects on the Fe($K\alpha$) peak intensity. The results showed an Fe to Nb ratio of $\frac{1}{3}$, corresponding to a chemical composition Fe_{0.25}Nb_{0.75}Se₃. From this, we can conclude that the composition of the crystals formed from starting powders with more than 10% iron was, in all cases, of the form Fe_{0.25}Nb_{0.75}Se₃.

X-ray powder patterns from reacted materials with the bulk composition Fe_xNb_{1-x}Se₃, support the conclusion that the resulting compound is essentially independent of the starting composition. Least-squares fits of lattice parameters to powder patterns from materials with $x = 0.25, 0.33, 0.50,$ and 0.67 produced virtually identical lattice parameters.

Resistance measurements were made using a standard four-probe technique, using soldered or silver-paint contacts. For the high resistance at low temperatures, both the current and voltage were measured with electrometers. Current densities were maintained at less than 10% of the cur-

rent necessary to induce sample heating. Susceptibility measurements were made using a Faraday balance susceptometer, described in Ref. 8. Samples for the susceptibility measurements were about 10 mg of selected single crystals, which were randomly oriented with respect to the magnetic field. The field dependence of the susceptibility shows no significant ferromagnetic contribution to the susceptibility, suggesting that the ion is divalent, t_{2g}^6 low spin $S = 0$.

The unit-cell parameters and crystallographic symmetry were obtained from standard x-ray precession and powder diffraction techniques, as discussed in Sec. II. CDW formation at low temperature was investigated by x-ray scattering using a high-intensity rotating anode x-ray source. Copper $K\alpha$ x rays were focused with a singly bent graphite monochromator, and a flat graphite analyzer was used on the diffracted beam. The resolution in this experiment was tighter than that used in a previous x-ray scattering study of NbSe₃,³ due to vertical Soller slits on the incident and the diffracted beam. This resulted in an in-plane resolution function with a full width at half maximum (FWHM) of 0.015 \AA^{-1} .

III. RESULTS

A. Electron transport and magnetic measurements

Resistance as a function of temperature for single crystals of Fe_{0.25}Nb_{0.75}Se₃ was measured and is shown in Figs. 1 and 2. The resistivity is 8×10^{-4} ohm cm at room temperature, corresponding to about the same value as that measured for pure NbSe₃. At about 100 K the resistance begins to rise as the temperature is decreased, and follows a very rapid functional form suggesting either an exponential or a power law. Detailed fits over the various temperature ranges will be discussed in Sec. IV. The resistance is Ohmic at electric fields up to 25 V/cm. The resistivity was also measured for a pure NbSe₃ crystal with a RRR = 230, as shown in Fig. 3(a), and for one of the single crystals with less than 1% iron, as shown in Fig. 3(b). Both of these crystals show the charge-density-wave anomalies at 59 and 145 K. The only significant difference is the decrease in the RRR of the iron-doped crystal. The pure NbSe₃ was also measured with low ac current densities ($J = 2.5 \text{ mA/mm}^2$), using phase-sensitive techniques in order to detect a superconducting transition. In contrast with previous measurements in pure NbSe₃,^{9,10} no resistive drop suggestive of superconductivity was observed down to 1.1 K.

Magnetic susceptibility as a function of temperature for Fe_{0.25}Nb_{0.75}Se₃ is shown in Fig. 4. Unlike

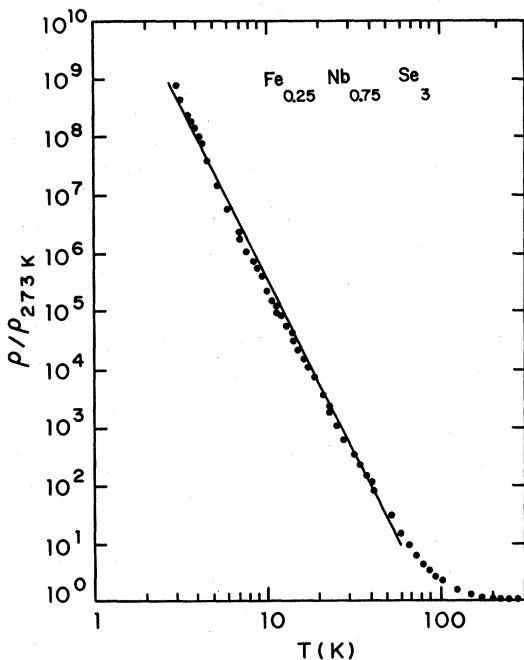


FIG. 1. Resistance versus temperature for $\text{Fe}_{0.25}\text{Nb}_{0.75}\text{Se}_3$ plotted on log scales showing the resistance increasing by nine orders of magnitude between 100 and 2.8 K. The solid line has a slope of 6.

NbSe_3 , the susceptibility is paramagnetic, with a room-temperature value of about 1.7×10^{-6} emu/gm. The susceptibility shows a minimum at about 180 K, with a slow increase with temperature up to 500 K. Below 180 K, the susceptibility increases as the temperature is increased and can be fit to a Curie-Weiss expression $\chi - \chi_0 = C/(T - \theta)$, where $C = \mu_{\text{eff}} N_i / 3k_B$, N_i = impurity concentration and $\mu_{\text{eff}} = g \mu_B [S(S+1)]^{1/2}$. This fit corresponds to either a very small μ_{eff} of about $0.1 \mu_B$ per iron atom,

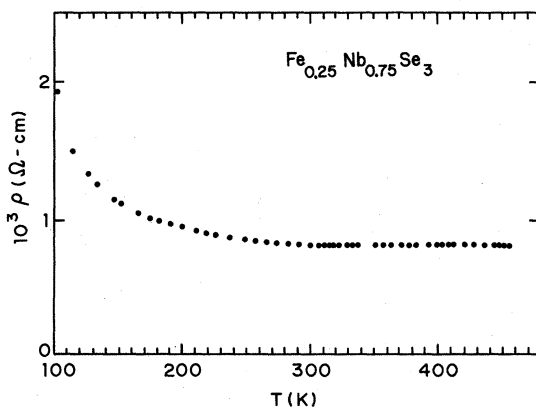


FIG. 2. Resistivity of $\text{Fe}_{0.25}\text{Nb}_{0.75}\text{Se}_3$ as a function of temperature above the resistive rise. The resistivity remains constant at high temperatures with a value of about 8×10^{-4} Ω cm.

or only a small number of iron atoms have a moment. If we assume spin values of between $\frac{1}{2}$ and $\frac{3}{2}$, then the Curie-Weiss behavior can be fit if N_i is about 1% of the iron atoms. This might be due to some iron atoms which are not incorporated into the $\text{Fe}_{0.25}\text{Nb}_{0.75}\text{Se}_3$ crystal in the regular lattice sites but in random impurity sites. The fact that there is little or no moment suggests that the iron may be in the Fe^{2+} state, t_{2g}^6 low spin $S=0$.

B. Structure

Crystallographic symmetry and approximate unit-cell dimensions of $\text{Fe}_{0.25}\text{Nb}_{0.75}\text{Se}_3$ were determined by single-crystal x-ray precession camera photographs. As in NbSe_3 , the unique axis, b , is parallel to the long ribbon dimension. Investigation of the reciprocal-lattice plane perpendicular to b indicated monoclinic symmetry with Laue group $C_{2h}(2/m)$. The cell is primitive, with systematic absences only for reflections of the type $0k0$, with $k \neq 2n$ due to the presence of a 2_1 screw axis. The space-group symmetry is therefore either centrosymmetric $C_{2h}^2(P2_1/m)$ or noncentrosymmetric $C_2^2(P2_1)$. Accurate unit-cell parameters were obtained from a powder sample by least-squares fitting 28 Bragg reflections observed in flat-plate powder diffraction diagrams made with Cr $K\alpha$ radiation. The unit-cell dimensions are given in Table I, along with the lattice parameters of pure NbSe_3 from Ref. 11. The indexed powder diffraction pattern is presented in Table II.

Although a full structural study is necessary to determine the atomic distribution in $\text{Fe}_{0.25}\text{Nb}_{0.75}\text{Se}_3$, we can propose a reasonable model for the structure based on the observed unit-cell dimensions and space group, and analogies with NbSe_3 and related compounds. The selenides and sulfides of Ta, Nb, and Zr of stoichiometry MX_3 form compounds in which the basic structural units are MX_6 triangular prisms.¹² The prisms share triangular end faces and form a characteristic chain structure parallel to one crystallographic axis. The number of chains per unit cell is even, and varies between two in ZrSe_3 and 24 in TaS_3 . The molecular volume is dependent on the size of the coordinate prisms and their packing density, and varies between about 96 \AA^3 in ZrSe_3 and 76 \AA^3 in NbSe_3 . Many of the compounds have been shown to be monoclinic, with space-group symmetry $C_{2h}^2(P2_1/m)$.

Based on this series of compounds and our observed unit-cell parameters, we propose that the majority of the iron in $\text{Fe}_{0.25}\text{Nb}_{0.75}\text{Se}_3$ is substituted directly for niobium in the six coordinated MSe_6 triangular prisms, and that there are four

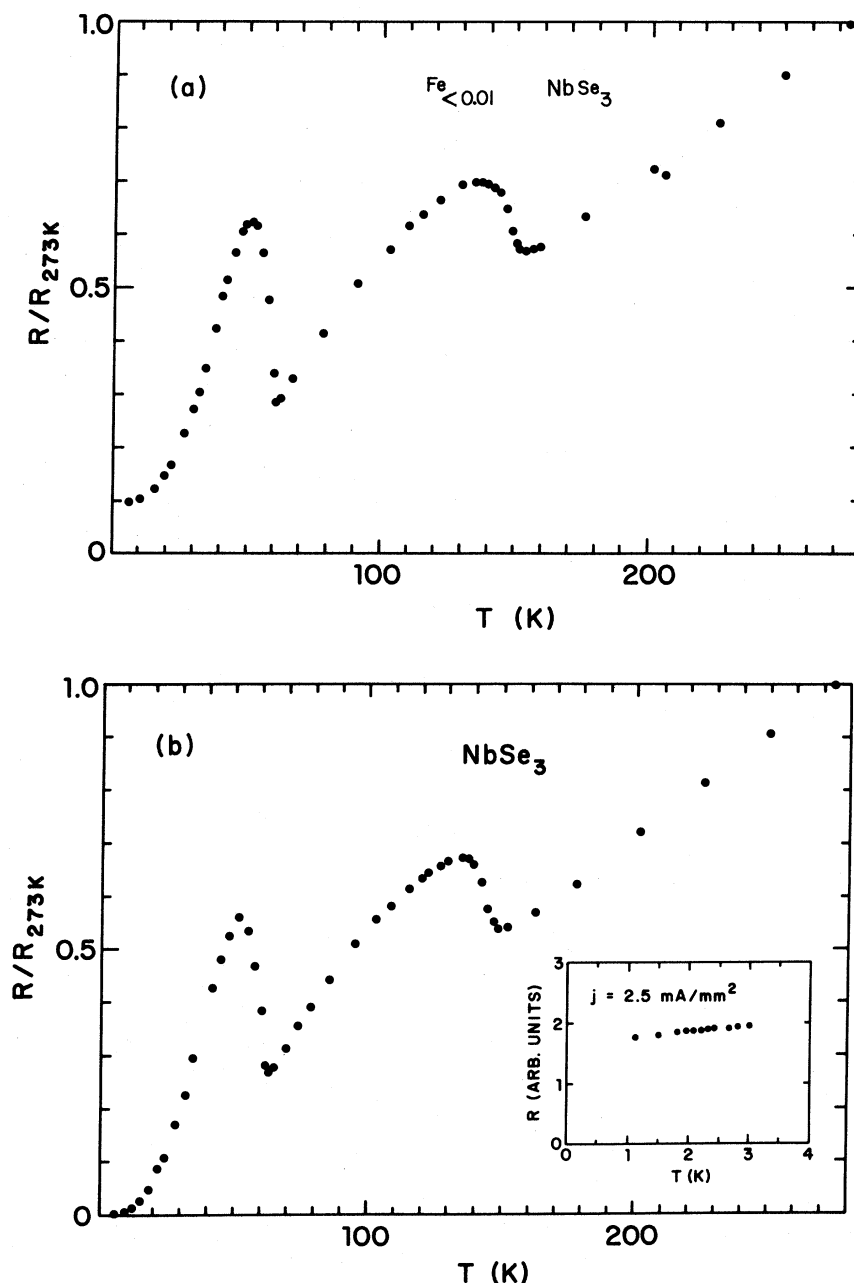


FIG. 3. (a) Resistance versus temperature of Fe_xNbSe_3 where $x < 0.01$, showing the charge-density-wave anomalies characteristic of $NbSe_3$. The residual resistance ratio of this sample is about 10. (b) Resistance versus temperature of $NbSe_3$ with a residual resistance ratio of 230. The insert shows the low-temperature measurement, using a low current density showing no detectable superconducting transition.

prism chains per unit cell. Iron occurs in six fold coordination in its two binary selenides, $FeSe$ and $FeSe_2$; however, the $FeSe_6$ coordination is octahedral. If the iron atoms in $Fe_{0.25}Nb_{0.75}Se_3$ forced the rotation of alternate triangular faces of the triangular prisms to form octahedra, then the monoclinic b axis would be double that of $NbSe_3$. The

fact that the b axis of $Fe_{0.25}Nb_{0.75}Se_3$ is virtually identical to that of $NbSe_3$ indicates that the iron assumes triangular prismatic coordination and alters the height of the MSe_6 prisms very little. Each unit cell of $NbSe_3$ contains six chains arranged in a two-by-three array with the long axis parallel to c . As shown in Table I, the length of the $Fe_{0.25}Nb_{0.75}Se_3$ c axis

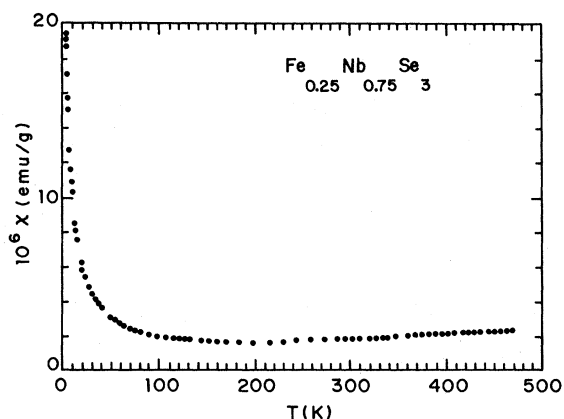


FIG. 4. Magnetic susceptibility versus temperature from 1.5 to 470 K. A small Curie-Weiss dependence is observed at temperatures below 100 K. The susceptibility is paramagnetic at all temperatures and increases as a function of temperature for temperatures greater than 200 K.

is very close to $\frac{2}{3}$ of the NbSe_3 c axis. We suggest that the $\text{Fe}_{0.25}\text{Nb}_{0.75}\text{Se}_3$ unit cell consists of four chains arranged in a two-by-two array. The resulting molecular volume of 75.0 \AA^3 is comparable to the lowest molecular volumes displayed by compounds in the NbSe_3 class. The only major dimensional difference then, between NbSe_3 and $\text{Fe}_{0.25}\text{Nb}_{0.75}\text{Se}_3$, is a shrinkage of the a -axis length of about 8% on iron incorporation.

Further, the observed space-group symmetry and unit-cell dimensions allow us to propose that iron is substituted for niobium at the centers of the triangular prisms in $\text{Fe}_{0.25}\text{Nb}_{0.75}\text{Se}_3$ in a disordered manner. For both of the proposed space groups (C_{2h}^2 and C_2^2), the screw axis requires that the prismatic chains occur in groups of two which are exactly equivalent. This means that any atom at a position (x, y, z) in the unit cell has an equivalent atom at $(\bar{x}, y + \frac{1}{2}, \bar{z})$. Thus, the possibility of having one chain with 100%-iron occupation is not allowed by symmetry. One could, in principle, have other ordered configurations where the iron is divided equally between two or four chains. Any ordering of this type, however, will result in a

TABLE I. Lattice parameters for $\text{Fe}_{0.25}\text{Nb}_{0.75}\text{Se}_3$ (this work) and NbSe_3 (Ref. 9).

	$\text{Fe}_{0.25}\text{Nb}_{0.75}\text{Se}_3$	NbSe_3
a	9.213(1) \AA	10.009 \AA
b	3.4773(9) \AA	3.4805 \AA
c	10.299(1) \AA	15.629 \AA
β	114.52(1) $^\circ$	109.47 $^\circ$

TABLE II. Comparison of observed and calculated interplanar spacings of $\text{Fe}_{0.25}\text{Nb}_{0.75}\text{Se}_3$ from powder diffraction data.

h	k	l	d_{calc}	d_{obs}
0	0	1	9.3695	9.3957
1	0	0	8.3816	8.4027
-1	0	1	8.1502	8.1696
1	0	1	5.2561	5.2602
-1	0	2	5.0861	5.0901
-2	0	1	4.6035	4.6060
2	0	0	4.1908	4.1927
-2	0	2	4.0751	4.0763
-1	0	3	3.4291	3.4290
-3	0	1	3.0459	3.0453
-3	0	2	3.0117	3.0097
-2	1	1	2.7747	2.7749
-3	0	3	2.7167	2.7170
-2	1	2	2.6452	2.6440
2	0	2	2.6280	2.6288
1	0	3	2.5953	2.5949
-1	0	4	2.5465	2.5458
-2	1	3	2.3654	2.3657
0	0	4	2.3424	2.3423
-4	0	2	2.3017	2.3014
3	1	0	2.1780	2.1780
-3	1	3	2.1408	2.1407
4	0	0	2.0954	2.0950
1	1	3	2.0799	2.0805
-1	1	4	2.0545	2.0548
-3	0	5	1.9829	1.9832
-5	0	1	1.7834	1.7835
0	0	7	1.3385	1.3385

superlattice along b ; that is, a two- or fourfold increase in the b -axis lattice parameter. We checked carefully for the presence of weak superstructure parallel to b and in the a - c plane. Long-exposure precession photographs and diffractometer scans at room temperatures in the $(hk0)$ zone showed no superlattice reflections. We therefore conclude that the iron is distributed randomly. On the basis of symmetry, the iron could be distributed randomly over all four chains or it could be divided only among two of the chains. Our measurements cannot distinguish between these two possibilities.

Since the conclusion of random iron sites depends upon the presence of a 2_1 screw axis, we carefully checked for the absence of scattering near $0k0$ -type reflections with $k \neq 2n$. Diffractometer scans along $0k0$ reveal weak intensity at (010) and (030) , which was about 10^{-3} of the allowed (020) intensity, but we also observed similar scattering at (010) and (030) in NbSe_3 where the 2_1 screw axis is well established by a structural study.¹¹ On the basis of a dramatic variation in the intensity which occurred when the sample was rotated about the (010) or (030) diffraction vectors,

we conclude that the $(0k0)$ intensity for $k \neq 2n$ is a result of multiple scattering in both compounds, and that the 2_1 screw axis in $\text{Fe}_{0.25}\text{Nb}_{0.75}\text{Se}_3$ is well established.

C. CDW formation

We now turn to a discussion of the low-temperature, x-ray scattering results. A previous x-ray scattering study³ showed that the two resistive anomalies in NbSe_3 are associated with two independent CDWs which produce phase transitions at $T_1 = 144$ K and $T_2 = 59$ K. The higher-temperature CDW results in a distortion parallel to the b axis with a reduced wave vector $\vec{q}_1 = (0, 0.243, 0)$, while the lower-temperature CDW has off-axis components and a reduced wave vector of $\vec{q}_2 = (0.5, 0.263, 0.5)$. The compound $\text{Fe}_{0.25}\text{Nb}_{0.75}\text{Se}_3$ has a weak, incommensurate CDW which forms at about 140 K with a distortion parallel to the b axis and a wave vector which is close to the value found in NbSe_3 . The reduced wave vector is slightly temperature dependent, with a value of $\vec{q} = (0, 0.27 \pm .003, 0)$ near 140 K and $\vec{q} = (0, 0.258 \pm .003, 0)$ near 6 K. Figure 5 shows scans along $(1k0)$ at a temperature of 6 K through the $(1, 1.74, 0)$ superlattice peak and the (120) peak of the host lattice. The $(1, 1.74, 0)$ superlattice peak is three times broader than resolution, with a FWHM of 0.040 \AA^{-1} , as compared with 0.013 \AA^{-1} for the (120) peak. Scans along $(1k0)$ and $(h, 1.74, 0)$ give inverse coherence lengths of $\kappa_{11}^{-1} \approx 50 \text{ \AA}$ and $\kappa_{12}^{-1} \approx 14 \text{ \AA}$ or an anisotropy of about 3.6. In the previous study of NbSe_3 ,³ the resolution FWHM was about 0.040 \AA^{-1} , so only a lower

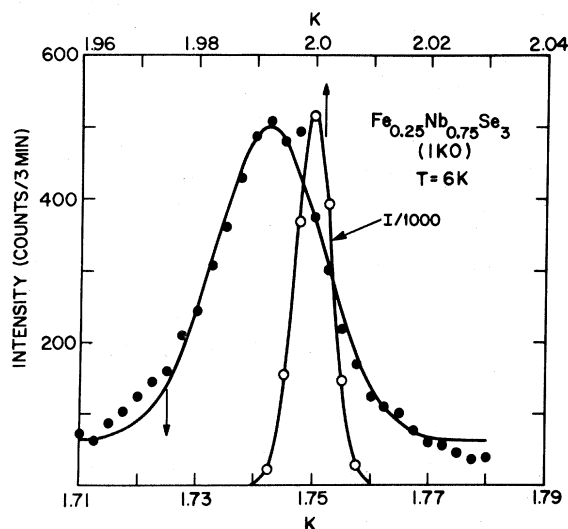


FIG. 5. Scans along $(1k0)$ through the (120) main Bragg peak and the $(1, 1.74, 0)$ superlattice peak. The superlattice peak is about three times broader than resolution, indicating an inverse coherence length of $\kappa^{-1} = 50 \text{ \AA}$.

bound of the low-temperature CDW coherence length was known. The anisotropy observed in diffuse scattering above the two-phase transition was about the same as reported in this work. The amplitude of the CDW in $\text{Fe}_{0.25}\text{Nb}_{0.75}\text{Se}_3$ is lower than in NbSe_3 , as evidenced by the intensities of the superlattice peaks relative to the main Bragg peaks, which are about a factor of ten less than in NbSe_3 . Figure 6 shows the integrated intensity of the $(1, 1.74, 0)$ superlattice peak as a function of temperature. The solid line is a guide to the eye. The data in Fig. 6 have been normalized to the intensity of the $(1, 1.74, 0)$ peak at 6 K and scaled to the intensity of the (120) Bragg peak at each temperature. The phase transition is broad and the order-parameter data show considerable rounding due to critical scattering near the phase transition. An extrapolation of the temperature dependence of the intensity at low temperature gives an onset value for the CDW of about 140 K, a value very close to that of the higher-temperature CDW, in NbSe_3 . No additional scattering was observed near reduced wave vectors of $\vec{q} = (0.5, 0.26, 0.5)$, corresponding to the low-temperature CDW in NbSe_3 .

An important question to resolve is the possibility that the observed superlattice is not intrinsic to $\text{Fe}_{0.25}\text{Nb}_{0.75}\text{Se}_3$. The fact that $\text{Fe}_{0.25}\text{Nb}_{0.75}\text{Se}_3$ has a CDW with nearly the same wave vector and transition temperature as NbSe_3 is remarkable, considering that the crystal structure is drastically altered. One therefore must consider the possibility that the observed superlattice intensities result from a phase mixture of NbSe_3 or a lightly doped alloy of NbSe_3 . The 8% difference between the a -axis lattice parameter of the iron-doped and the

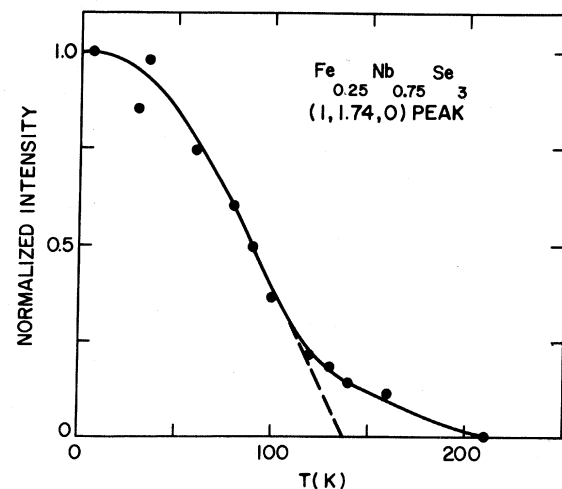


FIG. 6. Normalized intensity of the $(1, 1.74, 0)$ superlattice peak as a function of temperature. The phase transition is broad, with significant rounding due to critical scattering near the onset.

pure material makes it straightforward to test this hypothesis. If the superlattice resulted from a second phase the satellites would not be separated by exactly $\pm\vec{q}$ from the Bragg peaks of the $\text{Fe}_{0.25}\text{Nb}_{0.75}\text{Se}_3$ lattice and the discrepancy would be readily apparent at higher-order reflections. Scans through the $(8, \pm 0.26, 0)$ and the $(8, \pm 0.74, 0)$ superlattice positions verified that the superlattice is a modulation of the $\text{Fe}_{0.25}\text{Nb}_{0.75}\text{Se}_3$ lattice and does not result from a phase mixture. Furthermore, no d spacings corresponding to NbSe_3 could be identified in either the x-ray powder patterns, a pseudo-random powder pattern from a single crystal using a Gandolfi camera, or from the spectrometer scans.

IV. DISCUSSION

The rapid and continuous rise in resistance observed below 100 K in $\text{Fe}_{0.25}\text{Nb}_{0.75}\text{Se}_3$ has been fit to various functional relations for resistivity versus temperature, but no unique expression valid over the entire temperature range has been found. Below 19 K a dependence of the form $\rho \propto e^{(T_0/T)^m}$, with $m = \frac{1}{4}$, is obeyed fairly well, as shown by the straight-line portion of the lower curve in Fig. 7. This type of dependence can result from a hopping conductivity associated with a Mott-type¹³ transition, where $m = \frac{1}{4}$, or from an Anderson localiza-

tion,¹⁴ where m can have a value between $\frac{1}{4}$ and 1. Above 19 K, the curve clearly deviates from the $m = \frac{1}{4}$ power law, and other exponents or functional relations are required. The upper curve of Fig. 7 shows a plot of $\log \rho / \rho_{273}$ vs T^{-1} . In this case, the range between $T = 19$ K and $T = 100$ K can be approximated by a straight-line segment with slope $\Delta = 0.04$ eV, indicating the possibility of a gap with thermally activated conductivity of the form $\rho \propto e^{\Delta/2kT}$. For both plots in Fig. 7, a clear transition in the functional dependence is indicated in the neighborhood of 19 K.

The rise in resistivity is correlated with the onset of the weak superlattice observed in the x-ray studies at ~ 120 – 140 K. The formation of a gap associated with a charge-density wave could require an activated conductivity below the onset. However, the small amplitude of the observed CDW suggests that only a small fraction of the conduction electrons are involved in the CDW. In addition, below 19 K the gap would have to be quite temperature dependent, unless an additional localization of electronic states were present at low temperatures due to the random distribution of substitutional Fe.

In some respects, the behavior is similar to that observed by Sambongi *et al.*¹ for pure TaS_3 , where a Peierls transition was proposed as the explanation for the rapid resistance rise below 200 K. In that case, an abrupt resistance rise was observed near 200 K, followed by a region between 200 and 120 K where $\rho \propto e^{\Delta/2kT}$, with $\Delta = 0.15$ eV. Below 100 K, a saturation of resistance was observed which the authors suggested might have been an experimental limitation rather than intrinsic to the sample. A superlattice formation was observed by x-ray diffraction to develop below the onset temperature of 200 K. The q vector was determined to be $\sim 0.25 c^*$.

In the present experiments, the Fe appears to be incorporated in the crystal with an average of one substitutional Fe atom per unit cell. No long-range order due to Fe is detected by x rays, suggesting that the substitution at one of the four niobium sites per unit cell is random relative to different cells. This well determined concentration of random iron is produced at relative short sintering and crystal-growth times. The final crystals, as measured by transport, x-ray fluorescence and x-ray diffraction, show relatively little variation and are insensitive to initial Fe concentrations in the starting powder. Whether the kinetics are such that longer annealing times could produce additional order or other phases has been explored, but there seems to be one unique phase of $\text{Fe}_{0.25}\text{Nb}_{0.75}\text{Se}_3$ for the present preparation conditions.

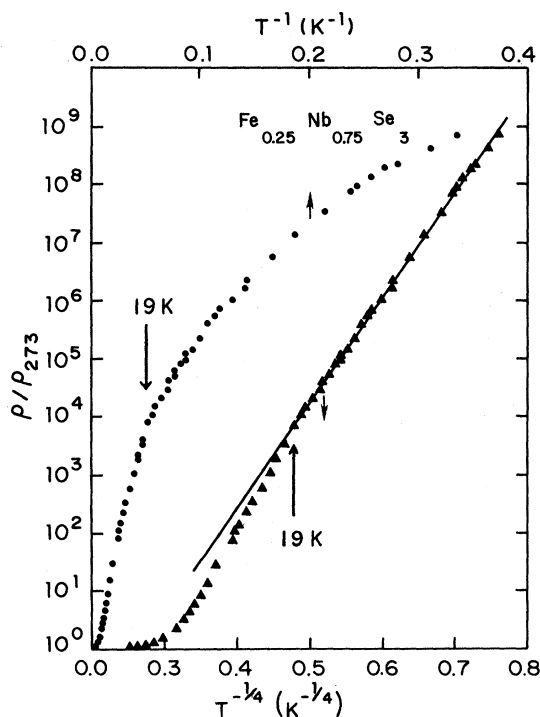


FIG. 7. Log of resistance for $\text{Fe}_{0.25}\text{Nb}_{0.75}\text{Se}_3$ vs T^{-1} (upper scale) and $T^{-1/4}$ (lower scale). The solid line shows a fit to the function $\rho \propto e^{T_0/T^{1/4}}$.

An extraordinary resistance rise^{6, 16} due to substitutional iron in a charge-density-wave material has also been observed in *IT*-TaS₂. In this case, the resistivity followed the empirical relation $\rho = \rho_0(T_0/T)^{a(x-x_c)}$, where a is a constant and x_c is a critical concentration. It was postulated⁶ that the charge-density wave present in the material produces an enhancement of the impurity localization by a local temperature-dependent CDW cloud. However, in the case of *IT*-Fe_xTa_{1-x}S₂, the functional dependence of the form $\rho \propto T^{-m}$ gives a value of $m = 2.5$. This can be clearly distinguished on $\log \rho$ vs T plots from functions of the form $\rho \sim e^{(T_0/T)^m}$, with m the range of values predicted for the usual type of metal-insulator transitions due to localization ($m = \frac{1}{4} - 1$). In the present data, a power law of the form $\rho \propto T^{-m}$ gives a value of $m = 6$, as indicated by the straight line in Fig. 1. This larger value of m makes it more difficult to clearly distinguish between the power-law and exponential behavior.

IT-TaSe₂ and *IT*-TaS₂ are similar in many ways to NbSe₃. They both have large resistance anomalies associated with the CDW formation and a relatively poor conductivity. If the charge-density wave is enhancing the localization, then both of these materials would be good systems in which to observe such effects.¹⁷⁻²⁰

There did not seem to be any correlation between the spin states of the metal dopants for the *IT* phases and the resistive changes. Therefore, the absence of a moment in Fe_{0.25}Nb_{0.75}Se₃ may play no role in the resistance transition. The fact that the susceptibility is paramagnetic for this system seems to indicate an increased Pauli paramagnetism, and therefore an increased conduction-electron density. This would tend to support the idea that the conduction electrons are being localized rather than the density being reduced

V. CONCLUSIONS

The incorporation of substitutional iron into NbSe₃ produces a unique new crystal structure with close to one iron atom for each three niobium atoms. The new structure has four chains of metal atoms per unit cell rather than six, as in pure NbSe₃. This structure is formed as single-crystal ribbons whenever the iron concentration of the starting material is above 10% of the niobium con-

centration. The unit cell is still monoclinic, with approximately the same b as in NbSe₃ but with substantially reduced a and c . The iron does not show any evidence of ordering and is randomly distributed in either two or four of the niobium chains.

X-ray studies show that a charge-density wave forms along the b axis below 140 K, with a reduced wave vector $\vec{q} = (0, 0.27, 0)$ near 140 K and $\vec{q} = (0, 0.26, 0)$ near 6 K. This is incommensurate with a q vector slightly greater than the commensurate value of $\vec{q} = 0.25 b^*$, in contrast to pure NbSe₃ where $\vec{q}_1 = (0, 0.24, 0)$ is slightly less than the commensurate value.

Below the onset of the charge-density wave, we observe a dramatic rise in resistance corresponding to nine orders of magnitude between 100 and 2.8 K. At temperatures below 19 K, this can be fit to the functional form characteristic of a Mott or Anderson type of metal-insulator transition characterized by electron localization. In the higher-temperature range, deviations occur and a more complicated temperature dependence is observed. The charge-density wave may produce a substantial enhancement of the metal-insulator transition and a local temperature-dependent charge-density-wave cloud can influence the precise temperature dependence.

The presence of the charge-density wave in the iron-doped material indicates that the Fermi-surface instability plays a dominant role in the electronic structure of the NbSe₃ compounds. It is quite surprising that the random potentials introduced by the iron do not quench the formation of the CDW but only weaken its amplitude. The crystal structure also undergoes a substantial modification, although the effective metal-atom chains along the b axis maintain a close similarity to those in pure NbSe₃.

ACKNOWLEDGMENTS

The authors wish to thank F. J. DiSalvo for helpful conversations and Estelle Phillips for valuable contributions to the UVa crystal-growth program. Professor R. Allen and Ms. M. Story provided help with the x-ray fluorescence analysis. We also wish to thank D. E. Moncton for the use of his x-ray scattering apparatus and J. V. Waszczak for help in sample preparation.

- ¹P. Monceau, N. P. Ong, A. M. Portis, A. Meerschaut, and J. Rouxel, *Phys. Rev. Lett.* **37**, 602 (1976); N. P. Ong and P. Monceau, *Phys. Rev. B* **16**, 3443 (1977).
- ²K. Tsutsumi, T. Takagaki, M. Yamamoto, Y. Shiozaki, M. Ido, T. Sambongi, K. Yamaya, and Y. Abe, *Phys. Rev. Lett.* **39**, 1675 (1977).
- ³R. M. Fleming, D. E. Moncton, and D. B. McWhan, *Phys. Rev. B* **18**, 5560 (1978).
- ⁴R. M. Fleming and C. C. Grimes, *Phys. Rev. Lett.* **43**, 1423 (1979).
- ⁵N. P. Ong, J. W. Brill, J. C. Eckert, J. W. Savage, S. K. Khanna, and R. B. Somoano, *Phys. Rev. Lett.* **43**, 811 (1979).
- ⁶F. J. DiSalvo, J. A. Wilson, and J. V. Waszczak, *Phys. Rev. Lett.* **36**, 885 (1976).
- ⁷R. M. Fleming, J. A. Polo, Jr., and R. V. Coleman, *Phys. Rev. B* **17**, 1634 (1978).
- ⁸S. J. Hillenius and R. V. Coleman, *Phys. Rev. B* **20**, 4569 (1969).
- ⁹R. H. Buhrman, C. M. Bastusch, J. C. Scott, and J. D. Kulick, in *Inhomogeneous Superconductors -1979*, Proceedings of the Conference on Inhomogeneous Superconductors, edited by D. U. Gubser, T. L. Franca-villa, S. A. Wolf, and J. R. Leibowitz (AIP, New York, 1980).
- ¹⁰P. Haen, F. Lapiene, P. Monceau, M. Núñez Regueiro, and J. Richard, *Solid State Commun.* **26**, 725 (1978).
- ¹¹J. L. Hodeau, M. Marzio, C. Roucau, R. Ayroles, A. Meerschaut, J. Rouxel, and P. Monceau, *J. Phys. C* **11**, 4117 (1978).
- ¹²A survey of the structure of the MX_3 family of compounds may be found in J. A. Wilson, *Phys. Rev. B* **19**, 6456 (1979).
- ¹³E. M. Hamilton, *Philos. Mag.* **26**, 1043 (1972).
- ¹⁴N. F. Mott, *Philos. Mag.* **19**, 835 (1969).
- ¹⁵T. Sambongi, K. Tsutsumi, Y. Shiozaki, M. Yamamoto, K. Yamaya, and Y. Abe, *Solid State Commun.* **22**, 729 (1977).
- ¹⁶R. M. Fleming and R. V. Coleman, *Phys. Rev. Lett.* **34**, 1502 (1975).
- ¹⁷P. D. Hambourger and F. J. DiSalvo, *Physica (Utrecht)* **99B**, 173 (1980).
- ¹⁸Y. Onuki, R. Inada, and S. Tanuma, *Physica (Utrecht)* **99B**, 177 (1980).
- ¹⁹P. Fazekas and E. Tosatti, *Physica (Utrecht)* **99B**, 183 (1980).
- ²⁰R. Inada, Y. Onuki, and S. Tanuma, *Physica (Utrecht)* **99B**, 188 (1980).